Viscosity of argon at temperatures > 2,000 K from measured shock thickness

Michael N. Macrossan and Charles R. Lilley

Center for Hypersonics, University of Queensland

Brisbane, Australia 4072

February 12, 2005

Abstract

Mott-Smith's approximate theory of plane 1D shock structure (*Phys. Rev.*, **82**, 885-92, 1951; *Phys. Rev.*, **5**, 1325-36, 1962) suggests, for any intermolecular potential, the average number of collisions undergone by a molecule as it cross the shock quickly approaches a limit as the Mach number increases. We check this with DSMC calculations and show that it can be used to estimate the gas viscosity at high temperatures from measurements of shock thickness. We consider a monatomic gas ($\gamma = 5/3$) for five different collision models and hence five different viscosity laws $\mu = \mu(T)$. The collision models are: the variable hard sphere, $\sigma \propto 1/g^{2\upsilon}$, with three values of υ; the generalized hard sphere; and the Maitland-Smith potential. For shock Mach numbers $M_1 \gtrapprox 4.48$, all these collision models predict a shock thickness $\Delta = 11.0\lambda_\mathrm{s}$, where λ_s is a suitably defined 'shock length scale', with a scatter $\approx 2.5\%$ (2 standard deviations). This shock length depends on the upstream flow speed, downstream density and a collision cross-section derived from the viscosity of the gas at a temperature T_g, characteristic of the collisions at relative speed $g = u_1 - u_2$ between upstream and downstream molecules. Using $\Delta = 11\lambda_\mathrm{s}$ and the experimental measurements of shock thickness in argon given by Alsmeyer (*J. Fluid Mech.* **74**, 498-513, 1976), we estimate the viscosity of argon at high values of T_g. These estimated values agree with the viscosity of argon recommended by the *CRC Handbook of Chemistry and Physics* (2001) at $T \approx 1,500$ K. For $T \gtrapprox 2,000$ K, for which there appears to be no reliable direct measurements of viscosity, our estimated values lie between the extrapolated values recommended by the *CRC Handbook* and those predicted by the simple power law $\mu = \mu_\mathrm{ref}(T/T_\mathrm{ref})^{0.72}$, with $T_\mathrm{ref} = 300$ K and $\mu_\mathrm{ref} = 2.283 \times 10^{-5}$ Pa.s. Taking the error in the experimental measurements of Δ as the scatter in the results of Alsmeyer ($\pm 2\%$), we estimate the uncertainty in the viscosity deduced from the shock thickness measurements as less than $\pm 5\%$. To this accuracy, our results agree with the power law predictions and disagree with the *CRC Handbook* values, for $T \gtrapprox 3,000$ K.
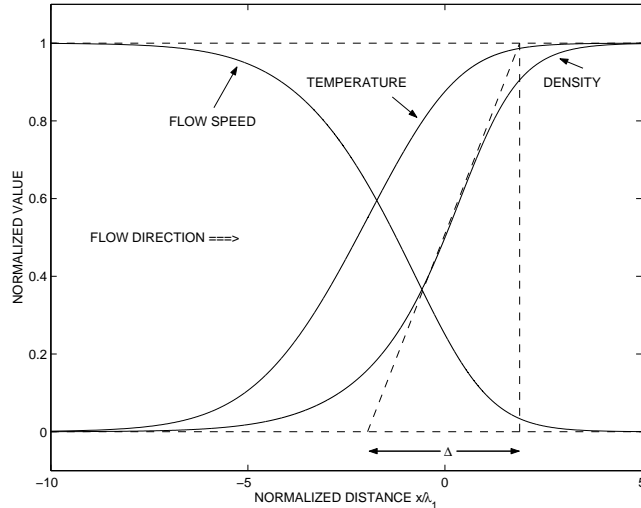
Figure 1: Normalized shock profiles, $(u - u_2) / (u_2 - u_1)$, $(T - T_1) / (T_2 - T_1)$, and $(\rho - \rho_1) / (\rho_2 - \rho_1)$ from solutions of Navier-Stokes equations for $M_1 = 3$, $\gamma = 5/3$ and $\mu = \mu_1 (T/T_1)^{0.72}$ (method of Ref. [1]). Shock thickness Δ from maximum density gradient.

1   Introduction

The internal structure of one dimensional shocks in a gas has been studied extensively, both experimentally and theoretically, to determine the viscosity law $\mu = \mu (T)$, and hence the intermolecular potential, for various gases. Gilbarg and Paolucci [1] gave a method for solving the Navier-Stokes equations numerically to obtain profiles of velocity, temperature and density through the shock, such as those shown in Fig. 1. A shock thickness can be derived from the density profile as

$$\Delta = \frac{\rho_2 - \rho_1}{d\rho/dx_{\max}},$$

where subscripts 1 and 2 denote the upstream and downstream conditions respectively, and where $d\rho/dx_{\max}$ is the maximum density gradient within the shock. The shock thickness of argon, a monatomic gas for which there are no complications arising from energy exchange between rotational, vibrational and translational modes, has been measured by various experimentalists [2], [3], [4]. Typical results for shock thickness, at various Mach numbers, obtained from the Navier-Stokes equations are shown in Fig. 2, for an assumed viscosity relation $\mu \propto T^{\omega}$, compared with the shock thickness measured in argon by Alsmeyer [4]. The figure also shows two curves fitted to the data, which are discussed below. The Navier-Stokes calculations under-estimate the shock thickness. However, for $\omega = 0.72$, the variation of Δ/λ_1 with M_1 is similar.[1]

Mott-Smith [5] found analytical solutions for shock structure based on an assumed bimodal velocity distribution within the shock. Mott-Smith found

---

[1] The data in Ref. [4] was presented in the form of λ_{HS}/Δ, where $\lambda_{HS} = 32\mu_1/(5\pi\rho_1\bar{c}_1)$ is the 'hard sphere' mean free path, which is different by a small constant factor from the nominal mean free path λ_1 of Eq. 4. We have made the appropriate conversion.
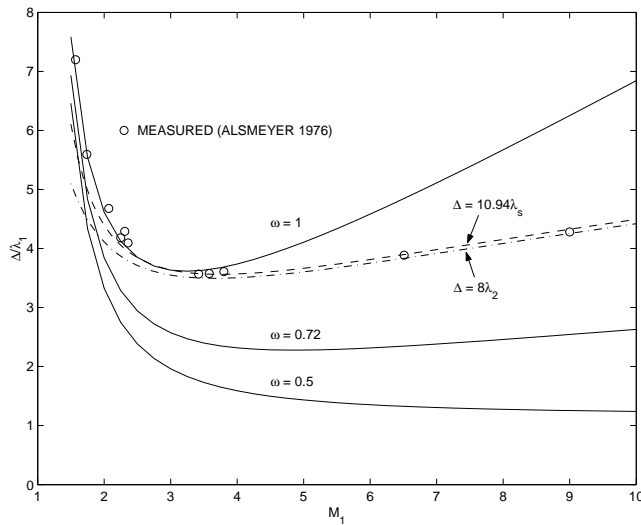
Figure 2: Normalized shock thickness Δ/λ_1 *vs.* M_1. Navier-Stokes calculations (method of Ref. [1]), $\gamma = 5/3$, $\mu = \mu_1 (T/T_1)^\omega$ with $\omega = 1, 0.72, 0.5$. Fitted curves: $\Delta = 10.94\lambda_s$ & $\Delta = 8\lambda_2$.

that, for this highly non-equilibrium distribution, the shock was thicker (the flow more dissipative) than predicted by the Navier-Stokes equations, and the results agreed better with experimental data. Muckenfuss [6] used the Mott-Smith method with various intermolecular potentials, and found that the average number of collisions suffered by a molecule as it traverses the shock approaches a limit for high M_1.

Macrossan [7] defined an approximate mean free path λ_{12} travelled by upstream particles (with mean speed u_1) penetrating a cloud of downstream particles (with number density, n_2 and mean speed u_2). This is given by

$$\lambda_{12} = \frac{u_1}{g\sigma_{12}n_2} = \left[\sigma_{12}n_2\left(1 - \frac{n_1}{n_2}\right)\right]^{-1}, \tag{1}$$

where

$$g = u_1 - u_2 = u_1\left(1 - u_2/u_1\right) = u_1\left(1 - n_1/n_2\right),$$

and the continuity equation $n_1u_1 = n_2u_2$ has been used. The effective collision speed is g and $\sigma_{12} = \sigma(g)$ is the collision cross-section at this speed, which was taken as the viscosity cross-section $\sigma_\mu(g) = 2\pi \int_0^\infty \sin^2\chi(b,g)\,b\,db$ for various collision models. Here χ is the deflection angle, which depends on the 'miss distance' b and the collision speed g [8]. Macrossan found that for an inverse power potential and for collision models having the same total cross-section as the inverse power potential, but different differential scattering laws, the shock thickness was an approximately constant multiple of λ_{12} for large M_1.

For real gases the viscosity cross-section $\sigma_\mu(g)$ is not known, so here we derive a value of $\sigma_{12}(g)$ for any viscosity law $\mu(T)$, by associating g with the average relative speed $(16RT/\pi)^{\frac{1}{2}}$ in an equilibrium gas at temperature T. This yields an equivalent 'collision temperature' at any collision speed g given

3

by
$$T_g = \pi g^2/16R. \tag{2}$$

The Chapman-Enskog viscosity [8] for hard sphere molecules, at this collision temperature, is

$$\mu(T_g) = \frac{5m}{16\sigma} (\pi R T_g)^{\frac{1}{2}}$$

where m is the molecular mass, and $\sigma = \pi d^2$ is the total cross-section. Thus the viscosity at temperature T_g can be used to derive an effective total cross-section at collision speed g as

$$\sigma(g) \approx \frac{5m}{16\mu(T_g)} (\pi R T_g)^{\frac{1}{2}} = \frac{5\pi}{64} \frac{mg}{\mu(T_g)}. \tag{3}$$

The cross-shock mean free path of Eq. 1 using $\sigma_{12} = \sigma$ from Eq. 3, becomes

$$\lambda_{12} \approx \left[\frac{5\pi}{64} \frac{mg}{\mu(T_g)} n_2 \left(1 - \frac{n_1}{n_2} \right) \right]^{-1}.$$

In terms of the *nominal* upstream mean free path

$$\lambda_1 = 2\mu_1/(mn_1\bar{c}_1) \tag{4}$$

where $\bar{c}_1 = (8RT_1/\pi)^{\frac{1}{2}}$ is the mean thermal speed, we have

$$\frac{\lambda_1}{\lambda_{12}} \approx \frac{5\pi^{\frac{3}{2}}}{64} S_1 \frac{\mu(T_1)}{\mu(T_g)} \frac{n_2}{n_1} \left(1 - \frac{n_1}{n_2} \right)^2,$$

where $S_1 = u_1/(2RT_1)^{\frac{1}{2}}$ is the shock speed ratio. It is convenient to drop the numerical constant $5\pi^{\frac{3}{2}}/64$ and define the 'shock length scale' as

$$\lambda_{\text{s}} \equiv \lambda_1 \left[S_1 \frac{\mu(T_1)}{\mu(T_g)} \frac{n_2}{n_1} \left(1 - \frac{n_1}{n_2} \right)^2 \right]^{-1}. \tag{5}$$

We expect the shock thickness to be a constant multiple of λ_{s} for strong shocks. Fig. 2 shows Alsmeyer's data [4] and a curve given by $\Delta = 10.94\lambda_{\text{s}}$, with an assumed viscosity for argon given by $\mu \propto T^{0.72}$. This fits the data for $M_1 > 3$ with a standard deviation of $< 1\%$. It is interesting to note that the shock length scale λ_{s} is approximately proportional to the downstream nominal mean free path $\lambda_2 = 2\mu_2/(\rho_2\bar{c}_2)$. Fig. 2 also shows the assumed relation $\Delta/\lambda_2 = 8$, again for $\mu \propto T^{0.72}$. This is not a best fit but was chosen for the sake of clarity in the figure.

We show in §4 that the thickness of strong shocks ($M_1 \gtrsim 4.48$) as calculated by DSMC, for a variety of different collision models (and viscosity laws) is given by

$$\Delta = 11\lambda_{\text{s}} \pm 0.28.$$

Assuming that this result would also be true for the real gas, the measured shock thickness for strong shocks can be used to *deduce* the gas viscosity at the temperature T_g. In the final section, therefore, we give values of argon viscosity for temperatures $1{,}500 \text{ K} \leq T \leq 6{,}000 \text{ K}$. There appears to be no other reliable experimental data for argon viscosity for $T \gtrsim 2{,}000 \text{ K}$.
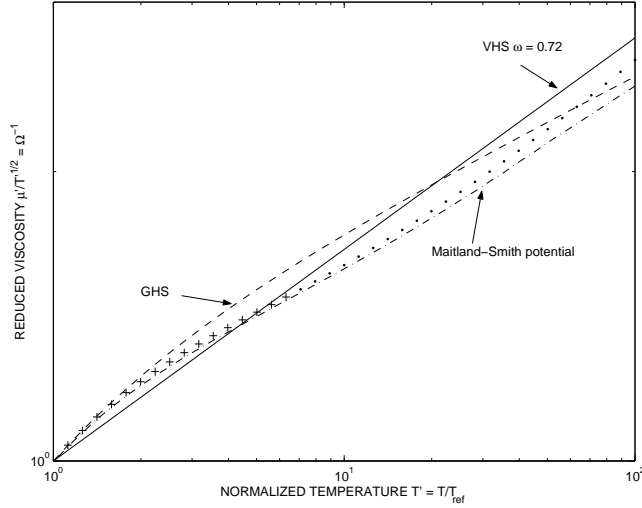
Figure 3: Reduced viscosity $\mu'/\sqrt{T'} = (\mu/\mu_{\mathrm{ref}})(T_{\mathrm{ref}}/T)^{\frac{1}{2}} = \Omega^{-1}$ *vs.* $T' = T/T_{\mathrm{ref}}$ for Argon. $\mu_{\mathrm{ref}} = 2.283 \times 10^{-5}$ Pa.s, $T_{\mathrm{ref}} = 300$ K. Recommended values: +, Kestin *et al.* [10] for $T < 2,000$ K and $*$, extrapolated for $T > 2,000$ K; Theoretical viscosity of VHS, $\mu = \mu_{\mathrm{ref}}(T/T_{\mathrm{ref}})^{0.72}$, GHS (Eq. 9) and Maitland-Smith (Eq. 11) collision models.

2   DSMC models and viscosity formulae

We use the DSMC method [9] to simulate the internal structure of a normal shock, with various collision models, and hence viscosity laws. It is convenient to express the viscosity in reduced form given by

$$\mu'\left(T'\right) = \mu\left(T\right)/\mu_{\mathrm{ref}}\left(T_{\mathrm{ref}}\right) = \sqrt{T'} \cdot \Omega\left(T'\right)^{-1}, \tag{6}$$

where $T' = T/T_{\mathrm{ref}}$ is a reduced temperature and $\Omega\left(T'\right)$ measures the departure of the viscosity law from the hard sphere law $\mu \propto T^{\frac{1}{2}}$. Eq. 6 can be rearranged as $\mu'/\sqrt{T'} = \Omega^{-1}$, which is used in Fig. 3 to show the various viscosity laws. The collisions models we considered are described below.

1. The variable hard sphere (VHS) molecular model has the same variation of cross-section with collision speed as an inverse power potential, but the scattering is isotropic. The Chapman-Enskog [8] approximation for its viscosity is

$$\mu = \mu_{\mathrm{ref}}\left(T/T_{\mathrm{ref}}\right)^{\omega}, \tag{7}$$

where ω is a constant and μ_{ref} is the viscosity at a reference temperature T_{ref}. We used ω values of 0.65, 0.72 and 0.81.

2. The GHS collision model [11] uses hard sphere scattering and a total collision cross-section made up of any number of VHS cross-sections. Here we use

$$\sigma/\sigma_0 = \phi\left(g_0/g\right)^{2v_1} + (1 - \phi)\left(g_0/g\right)^{2v_2} \tag{8}$$

where σ_0 is a reference cross-section, $g_0 = (4RT_0)^{\frac{1}{2}}$ and T_0 is a reference temperature. The Chapman-Enskog viscosity for this cross-section, (and

5

isotropic scattering), is

$$\mu = \frac{15\pi^{\frac{1}{2}}}{16\Gamma\left(4 - \upsilon_1\right)} \frac{\left(T/T_0\right)^{\frac{1}{2} + \upsilon_1}}{\left[\phi + (1 - \phi)S\right]} \frac{mg_0}{\sigma_0}. \tag{9}$$

where

$$S = \left(T_0/T\right)^{\upsilon_2 - \upsilon_1} \Gamma\left(4 - \upsilon_2\right) / \Gamma\left(4 - \upsilon_1\right).$$

As in Ref. [12], we use $(\upsilon_1, \upsilon_2, \phi) = (2/13, 14/13, 0.61)$. The cross-section $\sigma_0 = 6.425 \times 10^{-19}$ m^2 follows from Eq. 9 with $\mu_0 = 2.283 \times 10^{-5}$ Pa.s at $T_0 = 300$ K and $m = 66.3 \times 10^{-27}$ kg.

The GHS collision model can be extremely computationally inefficient; the collision probability increases dramatically for collision speeds $g <<$ $(4RT_0)^{\frac{1}{2}}$ so that an overwhelming number of low energy collisions must be calculated, even though these collisions make a negligible contribution to the viscosity behavior. To overcome this we use the modified GHS model [12], whereby the collision probability is independent of g for low values, in this case for $g/\left(4RT_0\right)^{\frac{1}{2}} \lesssim 1.035$. It can be shown that, for the values of υ_1, υ_2 and ϕ used, the viscosity of the modified GHS model is negligibly different from that in Eq. 9 for $T > 300$ K [12].

3. DSMC results of shock thickness in a monatomic gas were given by Erwin *et al.* [13], using the deflection angle in each collision calculated from the Maitland-Smith [14] potential

$$U(r) = kT_\epsilon \left[a_1 \left(\frac{r}{d}\right)^n - a_2 \left(\frac{r}{d}\right)^{-6}\right] \tag{10}$$

where

$$n = 13 + \xi\left(r/d - 1\right), \quad a_1 = 6/\left(n - 6\right), \quad a_2 = n/\left(n - 6\right) .$$

Here, r is the intermolecular separation, T_ϵ indicates the strength of the potential, d is the nominal molecular diameter and ξ is a constant. They used the values $T_\epsilon = 142.1$ K, $d = 3.76 \times 10^{-10}$ and $\xi = 7.5$ recommended for Argon in Ref. [15]. The upstream temperature in the simulations was $T_1 = 300$ K.

The Chapman-Enskog viscosity for the Maitland-Smith potential is given by

$$\mu = \frac{5m}{16\pi d^2} \frac{\left(\pi RT\right)^{\frac{1}{2}}}{\Omega^{(2,2)'}(T)} \tag{11}$$

where $\Omega^{(2,2)'}(T)$ is a weighted average of the viscosity cross-section [16]. The values of $\Omega(T)^{(2,2)'}$ given in the appendix of Ref. [15] for this potential appear to be too large by a factor ≈ 1.27. The values we calculate are given in Table 1.

With these values, and the molecular mass of argon, Eq. 11 gives excellent agreement with the Argon viscosity values recommended by Maitland and Smith [14], Kestin *et al.* [10] and Younglove and Hanley [17].

6

T'	$\Omega^{(2,2)'}$	T'	$\Omega^{(2,2)'}$	T'	$\Omega^{(2,2)'}$
0.1	2.9473	1.8	0.9586	12.0	0.6272
0.2	2.3791	2.0	0.9235	14.0	0.6116
0.3	2.0943	2.5	0.8605	16.0	0.5983
0.4	1.8882	3.0	0.8182	18.0	0.5868
0.5	1.7212	3.5	0.7877	20.0	0.5766
0.6	1.5836	4.0	0.7644	25.0	0.5553
0.7	1.4703	4.5	0.7457	30.0	0.5380
0.8	1.3767	5.0	0.7302	35.0	0.5234
0.9	1.2991	6.0	0.7055	40.0	0.5109
1.0	1.2341	7.0	0.6864	50.0	0.4901
1.2	1.1330	8.0	0.6709	60.0	0.4731
1.4	1.0588	9.0	0.6578	80.0	0.4469
1.6	1.0025	10.0	0.6463	100.0	0.4270

Table 1: Viscosity integral for the Maitland-Smith potential (Eq. 10).

3 Simulation method and data reduction

All simulations were performed using the normal shock simulation code DSMC1S, supplied by Bird [9], which uses the VHS model. The code was modified to use the GHS model also. The upstream temperature was $T_1 = 300$ K. Each simulation used 300 cells of length $< \lambda_1/5$, with six sub-cells per cell. The decoupling time step Δt was $\tau_2/5$ where τ_2 is the nominal collision time in the downstream flow. After an elapsed time $\approx 400\lambda_1/u_1$ to establish steady state, flow samples were taken at intervals of $5\Delta t$ until the sample sizes were typically $\sim 10^7$ particles per cell.

A typical density profile from the DSMC simulations is shown in Fig. 4. Although the profile appears smooth, the density gradient derived from it is not so smooth. Fig. 5 shows the two-point central difference estimate of the density gradient against location within the shock, as measured by the normalized density. There is some scatter in the results, particularly near the center of the shock where the gradient is greatest. Rather than use the two-point central difference gradient, we have taken the density gradient in each cell as the slope of the line of best fit to the density in five adjacent cells. This 'five-point' gradient is also shown in Fig. 5, where it can It can be seen that provides a reasonably smooth fit to the scattered two point central difference estimate. The shock thickness was obtained from the maximum five-point estimate of the density gradient.

4 Shock thickness

The calculated shock thicknesses for the various collision models are shown in Fig. 6. For the three VHS models the trends are similar to those found from the Navier-Stokes equations (Fig. 2). The GHS model and the Maitland-Smith potential give results which display a different trend from that for the
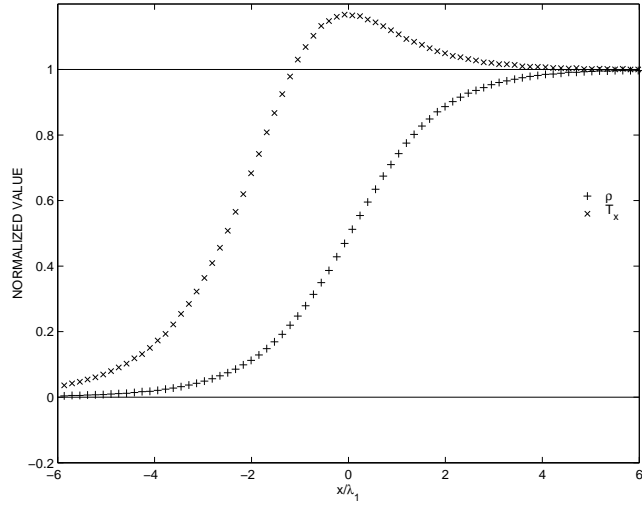
Figure 4: Normalized temperature $(T_x - T_1)/(T_2 - T_1)$ and density profiles $(\rho - \rho_1)/(\rho_2 - \rho_1)$ through shock. $M_1 = 2.5$. VHS collision model with $\omega = 0.72$. T_x is the x-component of translational temperature.
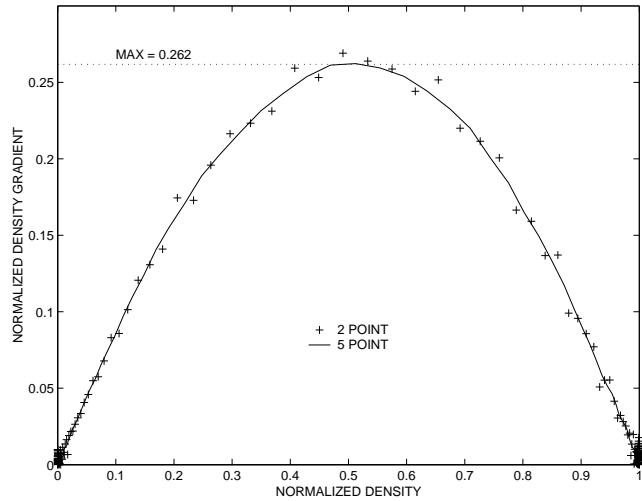

Figure 5: Normalized density gradient $\lambda_1 \left(d\rho/dx\right)/(\rho_2 - \rho_1)$ through the shock, from density profile shown in Fig. 4. Two-point central difference estimate and five-point estimate (gradient of line of best fit).
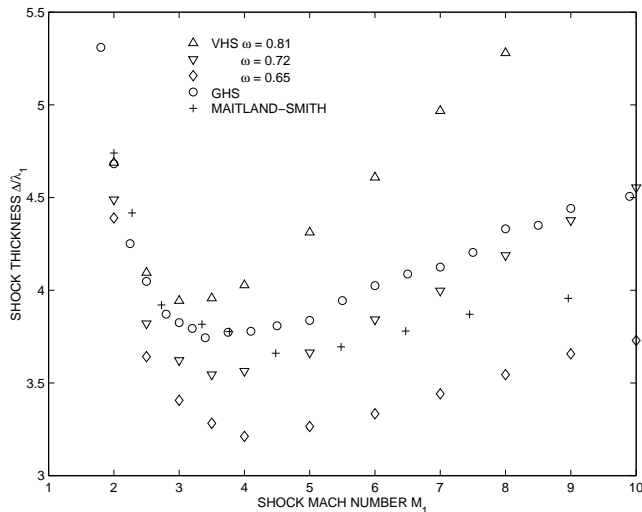
8

Figure 6: Shock thickness from DSMC simulations, for different collision models (viscosity laws). Maitland-Smith results from Ref. [13]

VHS models. We previously showed [18] that the value of Δ/λ_2 for various collision models approached a limiting value for strong shocks. This ratio is shown in Fig. 7 as a function of the downstream temperature T_2, rather than the shock Mach number. For $T_2 > 2,000$ K, all collision models have $\Delta = 8.3\lambda_2 \pm 0.5$, where the 'error' (0.5) is twice the standard deviation. Note that the individual collision models each approach a different limit and the deviation of one collision model about its corresponding limit is less than for the entire set. We previously [18] used this result and Alsmeyer's shock thickness measurements [4] to deduce the high temperature viscosity of argon. The error involved in this procedure was uncertain and due to the difficulty of establishing a limiting value of Δ/λ_2 for the unknown intermolecular potential (viscosity law) for the real gas.

No such problem exists if we use the data in the form of Δ/λ_s. As can be seen in Fig. 8, for $T_g > 1,000$ K, all the collision models produce a shock thickness $\Delta = 11.0\lambda_s \pm 0.28$, a deviation of less than 3%. It should be noted that the collision temperature of Eq. 2 was derived from the average relative speed of all pairs of molecules in a gas in equilibrium. We might have used the average relative speed in collisions, assuming a hard sphere cross-section (for example), to get $g = \Gamma(2.5)(4RT)^{\frac{1}{2}}$. Using this to define T_g, and hence λ_s, we find that the scatter in the values Δ/λ_s, for all collision models and $T_g > 2,000$ K, increases to 6% of the mean value. We reject this alternative and accept the value $\Delta/\lambda_s = 11 \pm 0.28$, for $T_g > 1,000$ K, with T_g given by Eq. 2.

5   Estimated high temperature viscosity

The results in Fig. 8 show that for any molecular model, Δ/λ_s tends towards a constant value, which may be denoted D_s, at high values of T_g. Taking
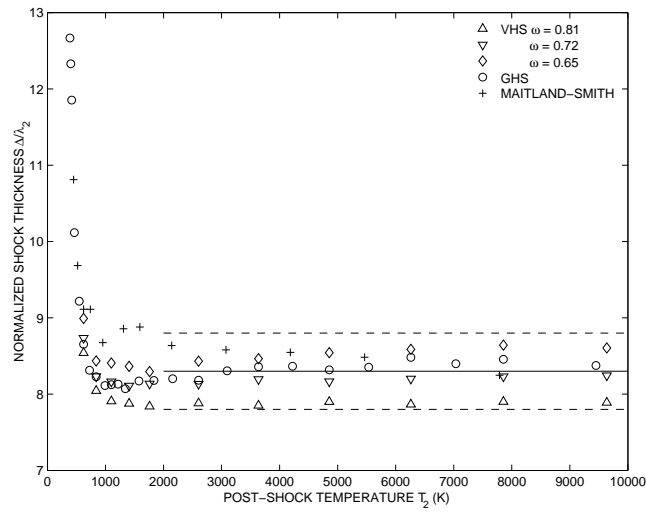
9

Figure 7: Shock thickness Δ/λ_2 *vs.* downstream temperature T_2. Results of DSMC simulations. Maitland-Smith results from Ref. [13]. For $T_2 \geq 2,000$ K, $\Delta/\lambda_2 = 8.3 \pm 0.5$ (2 s.d.).
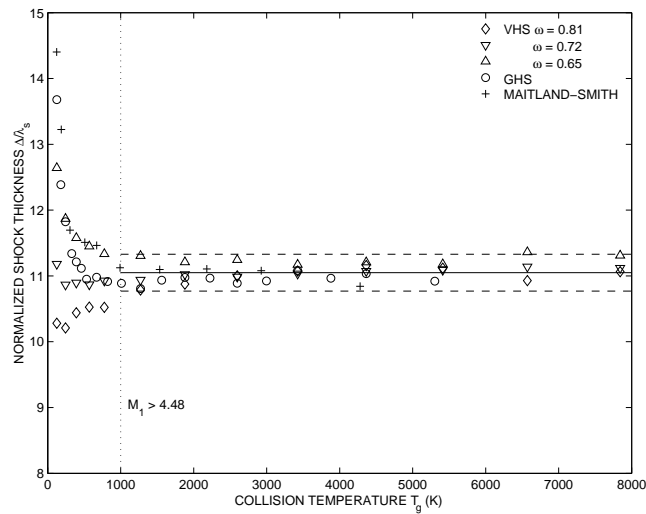

Figure 8: Shock thickness Δ/λ_s *vs.* collision temperature T_g of Eq. 2. Results of DSMC simulations. Maitland-Smith results from Ref. [13]. For $T_g \geq 1000$ K, $\Delta/\lambda_s = 11.0 \pm 0.28$ (2 s.d.).
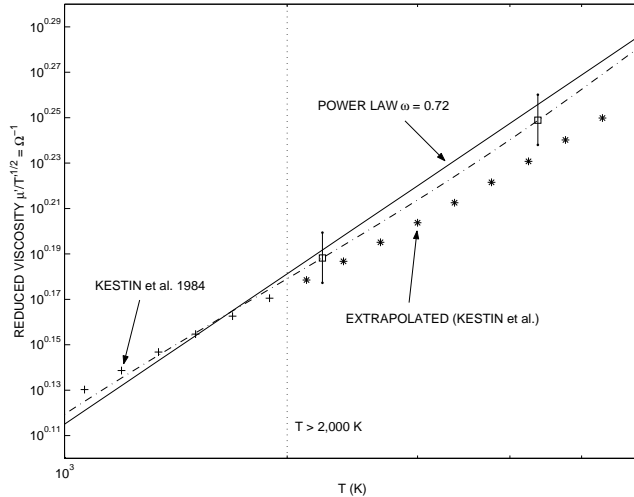
Figure 9: Reduced viscosity of argon, $\Omega^{-1} = \mu/\mu_{\text{ref}} (T_{\text{ref}}/T)^{\frac{1}{2}}$. $- \cdot \square -$ Present prediction from $\Delta/\lambda_1 \pm 2\%$, Ref. [4], and $D_{\text{s}} = 11 \pm 0.28$.

$D_{\text{s}} = 11$, we can use measured values of Δ to estimate the viscosity of the gas at temperature T_g. Thus, Eq. 5 gives

$$\Delta/D_{\text{s}} = \lambda_{\text{s}} = \lambda_1 \left[S_1 \frac{\mu(T_1)}{\mu(T_g)} \frac{n_2}{n_1} \left(1 - \frac{n_1}{n_2}\right)^2 \right]^{-1}.$$

This can be rearranged to give the viscosity at temperature T_g. Thus

$$\mu(T_g) = \frac{S_1}{D_{\text{s}}} \frac{n_2}{n_1} \left(1 - \frac{n_1}{n_2}\right)^2 \frac{\Delta}{\lambda_1} \mu(T_1). \tag{12}$$

The estimated viscosity, deduced from the strong shock results of Alsmeyer [4], is presented in Fig. 9 and Table 2. We have assumed that Alsmeyer performed all experiments at $T_1 = 300$ K. If we take the experimental uncertainty in Δ/λ_1 equal to the scatter of the measurements, which is 2%, we get a total uncertainty of less than $\pm 5\%$ for these viscosity predictions, when we allow for less than 3% uncertainty in the limiting value of D_{s}.

The *CRC Handbook of Chemistry and Physics* [19] recommends the use of argon viscosity values given by Kestin *et al.* [10] and Younglove and Hanley [17]. Kestin *et al.* give equations for viscosity that agree within 2.1% of 12 sets of experimental data over the range 100 K < T < 2,000 K. The recommended values are shown in Fig. 3. These values agree closely with those of Younglove and Hanley, and are probably more accurate than the earlier recommendations of Touloukian *et al.* [20]. Kestin *et al.* also recommend values of viscosity for $T > 2,000$ K, obtained from an extrapolation of a fitted equation. This extrapolation is also shown in Fig. 3 and in Fig. 9. The estimated viscosity in Table 2 agrees with the recommended values of Kestin *et al.* [10] at $T = 1,500$ K. For $T > 2,000$ K the present estimated viscosity lies between the predictions of the power law formula with $\omega = 0.72$, and the extrapolations of Kestin *et al.* For temperatures in the range 1,000 K to 6,000 K the present

11

M_1	5.40	6.18	6.5	7.50	8.63	9.0	9.62	10.52
Δ/λ_1 (Ref. [4])	3.75	3.84	3.89	4.03	4.21	4.28	4.39	4.55
T (K) (Eq. 2)	1,500	2,000	2,230	3,000	4,000	4,360	5,000	6,000
μ ($\times 10^5$ Pa s)	7.3	8.9	9.6	11.8	14.5	15.4	17.1	19.5

Table 2: Viscosity of argon deduced from $\lambda_\mathrm{s} = \Delta(\pm 2\%)/11(\pm 3\%)$.

estimates agree with the power law values to within 5%. For $T \gtrsim 3{,}000$ K, the present estimates are more than 5% larger than the extrapolations of Kestin *et al.*

It is possible that the value of D_s for the real gas (real intermolecular potential) lies outside the range $10.72 < D_\mathrm{s} < 11.28$ we found with the DSMC simulations. Also, there might be some systematic error in the experimental measurements of Δ. Both these possible errors could be eliminated if we scale the viscosity predictions given in Table 2, so that they agree with the recommended value given by Kestin *et al.* at some temperature at which we were convinced the recommended viscosity was most accurate. However since 1,500 K, the temperature at which our prediction already agrees with the recommended value, is close to the lowest temperature for which a constant value of D_s can be safely assumed (see Fig. 9) and is also close to the highest temperature for which the recommended value is reliably based on experimental data, there seems little point in adjusting our values to agree at some other temperature. We believe that the estimated uncertainty of less than 5% for the values given in Table 2 is reasonable.

6   Conclusions

We have defined a shock length scale λ_s proportional to the expected mean free path of molecules as they cross a shock, and have demonstrated using DSMC simulations, that the density-gradient thickness of strong shocks ($M_1 \gtrsim 4.48$) is given by $\Delta = 11\lambda_\mathrm{s} \pm 0.28$, regardless of the particular collision model (viscosity law). Using this result, and the shock thickness $\Delta \pm 2\%$ measured by Alsmeyer [4], the viscosity of argon has been estimated at temperatures that exceed the current limit of reliable experimental data at $T \sim 2{,}000$ K. The estimated viscosities at high temperatures are intermediate between the extrapolations given by Kestin *et al.* [10] and those predicted by the power law viscosity formula with $\omega = 0.72$. The estimated uncertainty in the values of viscosity given in Table 2 is less than 5%. For temperatures $> 3{,}000$ K, these values of viscosity are greater than the values given by Kestin *et al.* and agree with the power law predictions, to within the estimated uncertainty.

References

[1] D. Gilbarg and D. Paolucci. The structure of shock waves in the continuum theory of fluids. *J. Rat. Mech. Anal.*, 2:617–42, 1953.

[2] F. Robben and L. Talbot. Measurement of shock wave thickness by the electron beam fluorescence method. *Phys. Fluids*, 9(4):633–43, April 1966.

[3] B. Schmidt. Electron beam density measurements in shock waves in argon. *J. Fluid Mech.*, 39:361–73, 10th November 1969.

[4] H. Alsmeyer. Density profiles in argon and nitrogen shock waves measured by the absorption of an electron beam. *J. Fluid Mech.*, 74:497–513, 6th April 1976.

[5] H. M. Mott-Smith. The solution of the Boltzmann equation for a strong shock wave. *Phys. Rev.*, 82(6):885–92, June 1951.

[6] C. Muckenfuss. Some aspects of shock structre according to the bimodel model. *Phys. Fluids*, 5(11):1325–36, 1962.

[7] M. N. Macrossan. *Diatomic collision models used in the Monte-Carlo direct simulation method applied to rarefied hypersonic flows.* PhD thesis, Imperial College, University of London, 1983.

[8] S. Chapman and T. G. Cowling. *The mathematical theory of non-uniform gases.* Cambridge University Press, Cambridge, 3rd edition, 1970.

[9] G. A. Bird. *Molecular gas dynamics and the direct simulation of gas flows.* Clarendon Press, Oxford, 1994.

[10] J. Kestin, K. Knierim, E. A. Mason, B. Najafi, S. T. Ro, and M. Waldman. Equilibrium and transport properties of the noble gases and their mixtures at low density. *J. Phys. Chem. Ref. Data*, 13(1):229–303, 1984.

[11] D. B. Hash and H. A. Hassan. A generalized hard-sphere model for Monte-Carlo simulation. *Phys. Fluids A*, 5(3):738 – 744, March 1993.

[12] M. N. Macrossan and C. R. Lilley. Modified generalised hard sphere collision model for DSMC calculations. *J Thermophys Heat Trans*, 17:289–291, 2003.

[13] D. A. Erwin, G. C. Pham-Van-Diep, and E. P. Muntz. Nonequilibrium gas flows. I: A detailed validation of Monte Carlo direct simulation for monatomic gases. *Phys. Fluids A*, 3(4):697–705, April 1991.

[14] G. C. Maitland and E. B. Smith. Critical reassessment of viscosities of 11 common gases. *J. Chem. Eng. Data*, 17(2):150–6, 1972.

[15] G. C. Maitland, M. Rigby, E. B. Smith, and W. A. Wakeham. *Intermolecular forces: Their origin and determination.* Clarendon Press, Oxford, 1981.

[16] J. O. Hirschfelder, C. F. Curtis, and R. B. Bird. *Molecular theory of gases and liquids. (2nd ed.).* John Wiley and Sons, New York, 1965.

[17] B. A. Younglove and H. J. M. Hanley. The viscosity and thermal conductivity coefficients of gaseous and liquid argon. *J. Phys. Chem. Ref. Data*, 15(4):1323–37, 1986.

[18] C. R. Lilley and M. N. Macrossan. DSMC calculations of shock structure with various viscosity laws. In A. D. Ketsdever and E. P. Muntz, editors,

Rarefied Gas Dynamics: 23nd Int. Symp., Whistler, 2002. AIP Conference Proceedings 663, New York, Appendix (CD-ROM) 2003. Am. Inst. Phys.

[19] The Chemical Rubber Publishing Company. *CRC handbook of chemisty and physics*. CRC Press, Boca Raton, 82nd edition, 2001.

[20] Y. S. Touloukian, S. C. Saxena, and P. Hestermans. *Viscosity*, volume 11 of *Thermophysical properties of matter, the TPRC data series*. IFI/Plenum, New York, 1975.